Available online at www.eccomasproceedia.org
Eccomas Proceedia COMPDYN (2023) 2908-2916

ECCOMAS
Proceedia

COMPDYN 2023
9th ECCOMAS Thematic Conference on
Computational Methods in Structural Dynamics and Earthquake Engineering
M. Papadrakakis, M. Fragiadakis (eds.)
Athens, Greece, 12-14 June 2023

NUMERICAL BACK-ANALYSIS OF DYNAMIC CENTRIFUGE TESTS ON THE SEISMIC BEHAVIOUR OF CAISSON FOUNDATIONS SUPPORTING BRIDGE PIERS

Domenico Gaudio[1] **and Fabrizio Murillo**[2]

[1] University of Cambridge, UK (formerly Sapienza University of Rome, Italy)
High Cross, Madingley Road, Cambridge CB3 0EF, UK
e-mail: dg564@cam.ac.uk

[2] Politecnico di Milano
Piazza Leonardo da Vinci, 32, 20133 Milan, Italy
fabriziojose.murillo@mail.polimi.it

Abstract

Over the last few years, an ever-increasing interest on a sort of a "Reversed" Capacity Design of geotechnical systems has been emerging, particularly when looking at the seismic design of bridge foundations, such as shallow, piled and caisson foundations. In this approach, soil irreversible behaviour is triggered on purpose during strong seismic events, so as to protect the superstructure. Although the capacity of soil-caisson systems is quite high if compared to shallow and piled foundations, limit conditions of these systems may be actually attained during destructive seismic events.
The above-mentioned framework boosted the research on the dynamic response and interaction diagrams (i.e., failure envelopes) of rigid and massive caisson foundations [1][2]. Gaudio et al. [3] recently performed an experimental campaign via dynamic centrifuge tests, where a typical layout of a cylindrical caisson supporting a bridge pier was subjected to a series of ground motions. The caisson was embedded in a typical alluvial deposit, where the clay stratum was either soft and very soft.
In this paper, the results of preliminary 3D Finite Element back-analyses reproducing the centrifuge test are presented and discussed, for the specific soft-clay case. The analysis first aimed at reproducing and then extending the experimental investigation, so as to both validate and better understand the phenomena observed in the centrifuge. It is shown that, even with a simple but still comprehensive calibration of handy soil constitutive models, the main features ruling the seismic performance of the systems at hand can be fairly captured.

Keywords: Caisson Foundations, Soft clay, Centrifuge testing, 3D Finite Element Analyses, Dynamic Soil-Structure Interaction, Earthquakes.

ISSN:2623-3347 © 2023 The Authors. Published by Eccomas Proceedia.
Peer-review under responsibility of the organizing committee of COMPDYN 2023.
doi: 10.7712/120123.10609.20568

1. INTRODUCTION

It has been a long time since the engineering community realized that strong structure is not a synonym for safety when referring to earthquake-resistant systems. Nowadays, structural engineers rely on ductility for performing their designs. Nearly all the building codes worldwide allow plastic deformations to happen in focalized elements, reducing stresses in the critical ones, thus preventing collapse. Nonetheless, this concept is seldom applied to foundations.

Over the last decade, several studies have been performed to assess the effects of soil plasticity and soil-structure interaction on the performance of bridge piers under seismic actions. Studies like [4] and [5] showed that the inelastic behaviour of soils and the temporal attainment of bearing capacity could improve the performance of pier-deck systems. Following this framework, developments have been made concerning the "Reversed Capacity Design" (weak foundation-strong column) [6].

Most of these studies made use of numerical methods, taking advantage of the ongoing development of computational resources. However, commercial codes often rely on strong assumptions which may not correctly reproduce the system behaviour, whereas centrifuge experiments are more realistic but rarely available. This is why validation of the numerical models against centrifuge experiments is essential.

In this study, the centrifuge experiment performed by Gaudio *et al*. [3] is reproduced in the Finite Element (FE) code Plaxis 3D CE 2022 [7], where a caisson-pier-deck system embedded in a typical alluvial deposit with soft clay is subjected to a moderate-intensity earthquake. The comparison of the numerical results against the experimental ones shows that the main features ruling the seismic performance of the system may still be captured if a proper calibration of soil constitutive parameters is carried out.

2. PROBLEM LAYOUT

The study considers a typical configuration of a highway bridge pier, where the interaction with adjacent piers is neglected thanks to the assumption of a long span (L = 50 m). The pier consists of a circular concrete column of diameter d = 2.2 m and height h_s = 15 m, subjected to the self-weight of the concrete deck.

Figure 1 shows the problem layout. The pier-deck system is supported by a massive cylindrical concrete caisson with a diameter D = 8 m and height H = 8 m (slenderness ratio H/D = 1). The whole system is embedded in a typical alluvial deposit, consisting of a shallow 3-m-thick layer of loose sand overlying a 14-m-thick soft clay layer. The water table is located at the contact between the sand and clay, and the initial pore water pressure is hydrostatic.

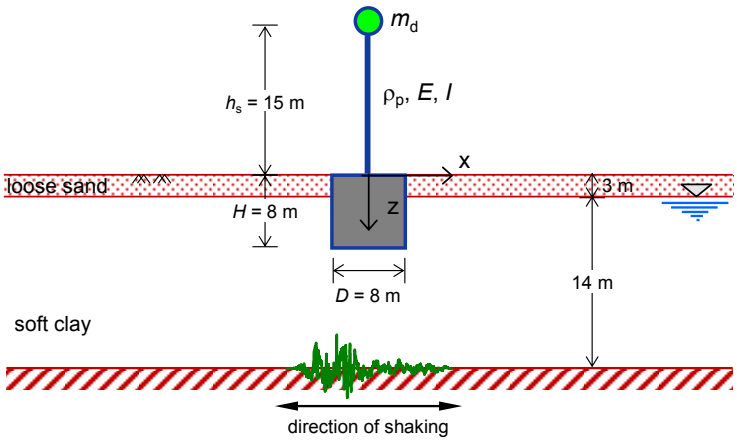

Figure 1: Schematic layout of the problem at prototype scale (modified from [8]).

For simplicity, the deck is assumed to be reproduced by a tip mass of m_s = 194.40 Mg. The total mass of the caisson is m_c = 1024.78 Mg, while the mass of the pier is m_p = 143.64 Mg with a bending stiffness EI = 30.7 GN·m^2, where E and I are Young modulus and cross-sectional moment of inertia, respectively. The system is subjected to ground motion at the bedrock depth (z = 17 m), here represented as a horizontal acceleration time history.

Figure 2 shows a schematic view of the centrifuge model reproducing the prototype. The model was scaled down according to the laws reported in [9] for a centrifugal acceleration of 60g. To correctly reproduce the prototype model, aluminum was used (alloy 6028-T6) with unit weight γ_{al} = 27 kN/m^3 both for the caisson (hollow cylinder) and the pier (rod). A brass cylinder (alloy CZ121) with γ_{br} = 85.6 kN/m^3 was adopted to simulate the deck as a lumped mass. The sand layer was made of Hostun Sand with a relative density D_R = 50%, while the clay layer was prepared from speswhite Kaolin powder. The physical and mechanical properties of the clay are listed in Table 1, where w is the water content, which was measured right before spinning up the model in the centrifuge, w_L, w_P are the liquid and plastic limits, $PI = w_L - w_P$ is the plasticity index, λ and κ are the slopes of the Normal Compression and of the Unloading–Reloading Lines in the semi-logarithmic v–p' (log) plane, and Γ and M are the intercept and the slope of the Critical State Line in the v–p' (log) and q–p' plane, respectively, with Γ being computed at p' = 1 kPa. The clay was consolidated at a stress level so that to obtain a soft clay (σ'_{vc} = 512 kPa), together with suction applied at the bottom, u = – 90 kPa. The model was placed into an Equivalent Shear Beam container (ESB) [10], whose dynamic boundary effects have been recently assessed [11]. In addition, the model was equipped with miniaturized instruments, such as those shown in Figure 2. The system was subjected to both recorded and sinusoidal time histories of the horizontal accelerations along the x-direction only, spanning a vast range of frequency contents and intensity levels, with peak accelerations ranging from 0.02g (*weak*) to 0.21g (*strong*). In this paper, reference to the Adana record is only made for the sake of brevity, which was characterised by a peak horizontal acceleration $a_{max, inp}$ = 0.133g (*moderate* intensity).

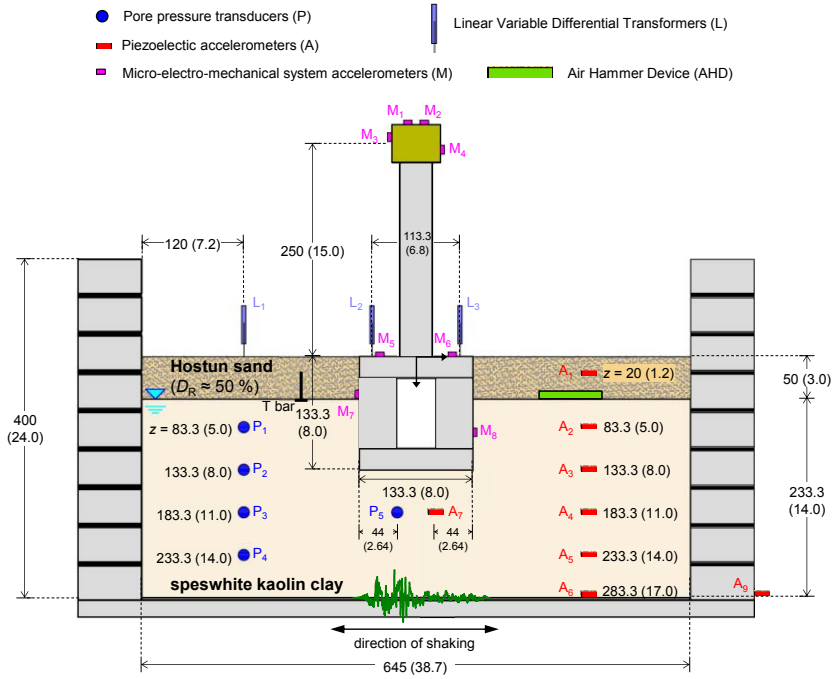

Figure 2: Elevation view of the centrifuge model at model scale (in mm) (bracketed prototype units: m) (modified from [8]).

w (%)	w_L (%)	w_P (%)	PI (%)	G_s (-)	Γ (-)	λ (-)	κ (-)	M (-)
56	58	34	24	2.61	2.87	0.14	0.03	0.80

Table 1: Properties of the speswhite Kaolin clay adopted in the centrifuge tests (modified from [3]).

3. 3D NUMERICAL MODEL

A 3D FE model was implemented in the code Plaxis 3D [7] to simulate the centrifuge model shown in Figure 2 at the prototype scale. Thanks to the symmetry of the problem, just half of the ESB box domain was modelled, leading to the dimensions reported in Figure 3. The sand and clay layers were subdivided into multiple sub-layers with thickness ranging from 1 to 3 m, with the thinner layers located in the shallow 10 m. This was made with a twofold objective: first, to reproduce the variability with depth of the mechanical properties of the soil deposit, and second, to guide the automatic mesh refinement performed by the software, so as to limit the numerical distortion of shear waves propagating into the FE domain [12]. To this end, the seismic input motion was applied a low-pass filter with a maximum frequency f_{max} = 8 Hz.

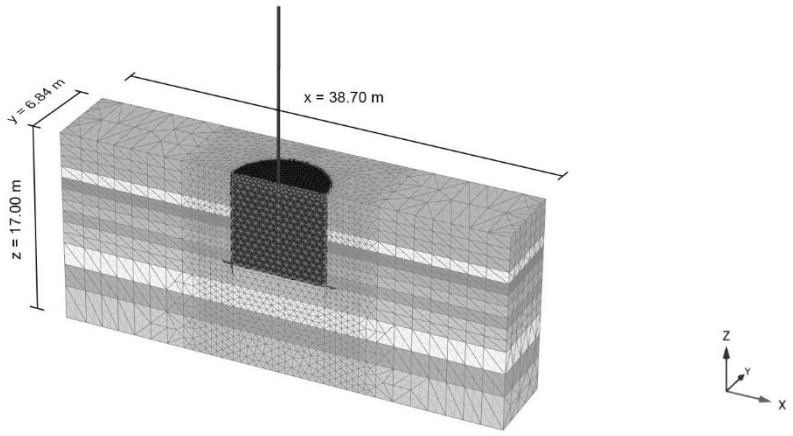

Figure 3: 3D FE model implemented in Plaxis 3D [7]

The soil and the caisson volumes were both modelled using 10-node tetrahedra, while the pier and the deck were modelled with *beam* elements. A very short beam element was adopted for the deck in order to reproduce a lumped mass. Finally, a rigid plate element was introduced atop the caisson to impose the continuity constraint between the beam element representing the pier and the tetrahedra simulating the caisson. The mesh was generated using the *coarse* option with a local coarseness factor equal to 0.2 for the volumes close to the caisson and to 1.5 for the farther ones, so that the desired mesh refinement was obtained (Fig. 3), which brought to 51225 elements and 75279 nodes.

In the static phases preceding the dynamic calculation, namely the k_0-procedure to initialise the lithostatic stress state and the *wished-in-place* activation of the caisson and the pier in drained conditions, the normal displacements were fixed along all the boundaries, and the horizontal displacement was also fixed at the bottom of the model ($u_x = u_y = 0$); the ground surface was assigned no restraint. Periodic boundaries (*i.e.,* tied-nodes) were adopted for the fully-undrained dynamic analysis, which means that the differential horizontal displacement between two nodes at the same depth along the vertical edges of the model was impeded ($\Delta u_x = 0$): this boundary condition allowed to mimic the dynamic boundary condition applied to the soil sample by the end walls of the ESB container, which are flexible and designed on the purpose of accommodating the deformation of an average dense/consistent soil deposit [10].

Both the structure and the caisson foundation were assigned non-porous linear-elastic materials, whereas the *HSsmall* constitutive model [13] was adopted for the soil layers.

The soil mechanical parameters were calibrated against those obtained in the centrifuge tests reported in Gaudio *et al*. [3]. First, the unit weight of the clay, γ, was obtained to reproduce the *in-flight* vertical effective stress profile, σ'_{v0}, which was measured before applying the ground motions: here it is worth mentioning that the stress state was affected by some residual excess pore water pressures in the clay, Δu, as the duration of consolidation preceding the dynamic phase did not last enough (1 hour only) to make Δu dissipate completely. These Δu were recorded at some specific depths with the Pore Pressure Transducers (PPT) (black crosses in Fig. 4a). Then, the OverConsolidation Ratio, *OCR*, was imposed to the different soil strata subdividing the clay layer (Fig. 4b). Moreover, the parameters ruling the small-strain shear modulus G_0, G_0^{ref} and m, were calibrated to fit the values computed from the Air Hammer (AH) test, both for the sand and the clay layers (Fig. 4c), according to the equation

$$G_0 = G_0^{ref}\left(\frac{c'\cot\varphi' + \sigma'_3}{c'\cot\varphi' + p^{ref}}\right)^m \tag{1}$$

where c' and φ' are the effective cohesion and angle of shearing resistance, respectively, σ'_3 is the minimum effective stress and $p^{ref} = 100$ kPa is a reference pressure. As for the clay, the effective cohesion c' was calibrated in order to provide the undrained shear strength s_u shown in Fig. 4d, providing a fair estimation of the experimental one, which in turn was measured with the T-bar penetrometer [14].

The remaining soil parameters are listed in Table 2, where the shear strain $\gamma_{0.7}$ was determined from the shear modulus decay curves, $G/G_0(\gamma)$, proposed in the literature ([15] for the sand and [16] for the clay layer), while moduli E_{ur}^{ref} and E_{oed}^{ref} were retrieved based on κ and λ reported in Table 1, respectively. A typical Poisson ratio ν_{ur} was assumed, and the elasto-plastic modulus E_{50}^{ref} was computed based on typical ratios ($E_{50}^{ref}/E_{oed}^{ref} = 1.00$ for the sand and 1.25 for the clay). Both the sand and the clay were assigned a null dilatancy angle ($\psi = 0$), together with the default value $R_f = 0.9$.

All materials adopted in the analyses were also assigned a damping ratio $\xi = 1$ % to damp out the response of the system at very low strains, as the *HSsmall* model does not provide any hysteretic damping in the small-strain range ($\gamma = 10^{-4}$ %).

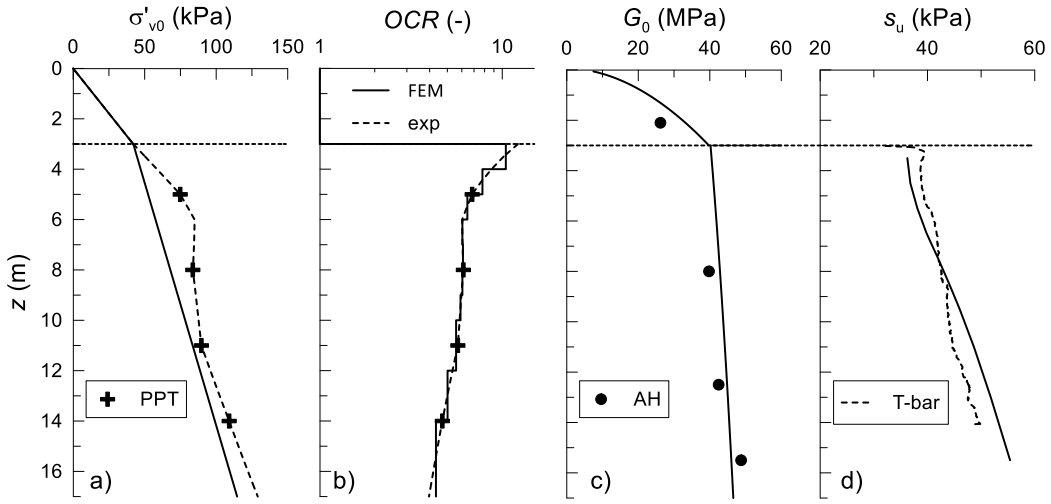

Figure 4**:** Calibration of the constitutive soil model: (a) effective vertical stress, (b) over consolidation ratio (c) initial shear modulus, and (d) undrained shear strength profiles.

soil	γ (kN/m^3)	G_0^{ref} (MPa)	m (-)	$\gamma_{0.7}$ (%)	E_{ur}^{ref} (MPa)	ν_{ur} (-)	E_{50}^{ref} (MPa)	E_{oed}^{ref} (MPa)	c' (kPa)	φ' (°)
sand	14.0	92.1	0.52	0.024	110.7	0.25	36.9	36.9	0.5	32.3
clay	15.0	45.5	0.23	0.044	11.4	0.25	2.2	1.7	15.0	20.7

Table 2: Mechanical parameters adopted in the *HSsmall* constitutive model.

4. NUMERICAL VS. EXPERIMENTAL RESULTS

In this section, the numerical results obtained from the fully-undrained dynamic calculation phase are compared to those from the centrifuge test. In particular, the time histories of the dimensionless deck drift (u_{rel}/h_s) are plotted in Fig. 5a, where the deck drift is defined as $u_{rel} = u_d - u_c$, with u_d and u_c being the deck and caisson horizontal displacement; in the same figure, the rigid rocking component ($tan\theta$) and the bending moment recorded at the base of the pier (M_s) are also plotted (Fig. 5b-c). The moment-rotation and relative settlement-rotation loops are also shown in Fig. 5d-e, where the moment was computed as follows:

$$M_s = m_{eff} \cdot a_d \cdot h_s \tag{2}$$

where $m_{eff} = 270.4$ Mg is the effective mass related to the first mode of the pier [3], while the relative settlement w_r was calculated as

$$w_r = w - w_{ff} \tag{3}$$

where w is the average settlement of the caisson, and w_{ff} is the settlement at the ground surface of the far-field alignment, which was measured with LVDT L1 in the centrifuge test (see Fig. 2).

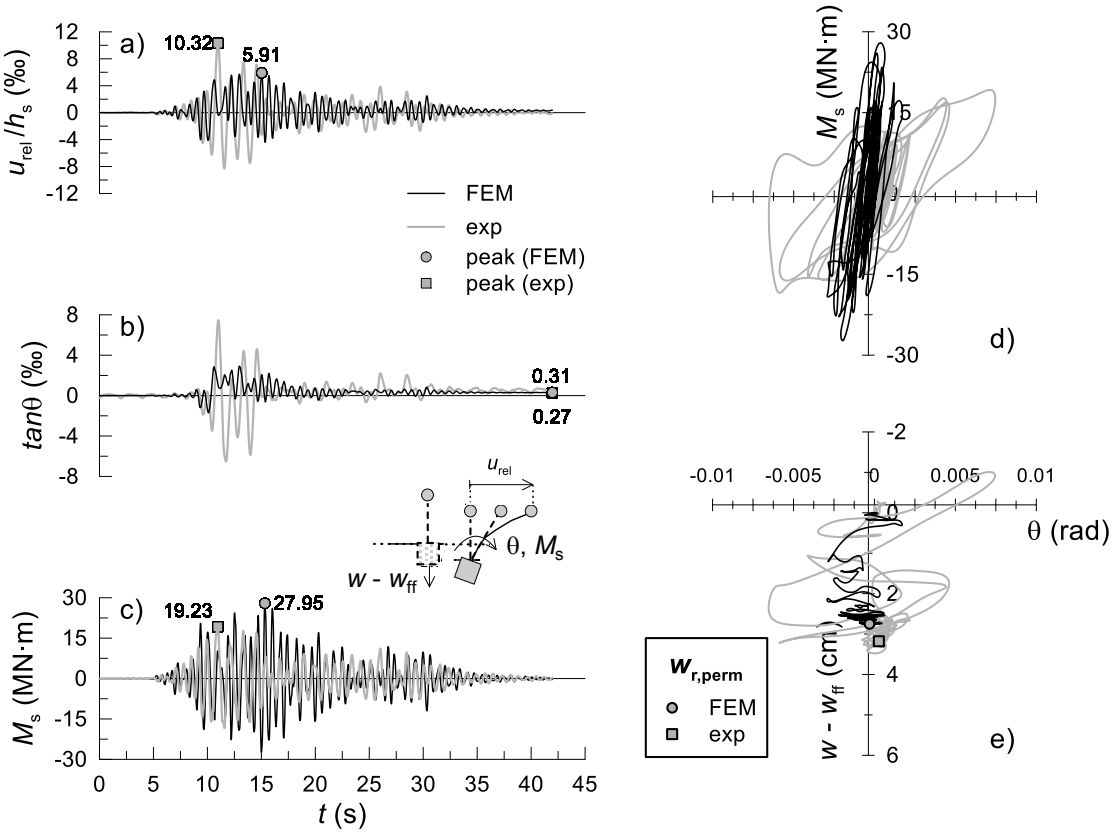

Figure 5: Time histories of the (a) total and (b) rigid component of deck drift, and of the (c) bending moment experienced by the system; (d) moment-rotation and (e) settlement-rotation loops.

The FE model provides a response which is stiffer than the experimental one, as it can be clearly seen in Figure 5a-d, where lower peak values of the deck drift and its rigid component are obtained, as a counterpart of the higher peak moment transmitted to the caisson. The frequency content of the time histories are quite similar though, which means that the period of the whole system is fairly captured by the numerical model. Moreover, permanent deformations, here expressed in terms of permanent tilting and settlement, are accurately reproduced in the FE analysis (Fig. 5e). As for these permanent values, it is worth noting that quite low values were computed, namely $tan\theta \sim 0.3$ % and $w_r \sim 3$ cm ($w_r/D \sim 0.4$ %), which clearly indicates that the system behaviour fell into the nonlinear elastic regime: the role of soil plasticity can be therefore deemed negligible, for the case at hand. This mostly holds true for the centrifuge test, where a broader area of the M_s-θ loop is observed, which entails more energy being dissipated in the soil deposit (Fig. 5d).

The comparison was also made in terms of the peak accelerations obtained at the far field, the caisson and the deck (Fig. 6). In the graphs, the results obtained in the centrifuge after applying the entire series of base excitations are reported, so as to provide the whole range of input accelerations $a_{max,\,inp}$ spanned during the test. The FE model provided a much higher acceleration at the far field (Fig. 6a): this is also true for the acceleration measured at the deck level (Fig. 6c), whereas a good agreement was obtained as for the caisson acceleration (Fig. 6b).

A much better agreement was achieved in terms of specific seismic performance indices [17], as reported in Figure 7. Here, the maximum and permanent drift of the deck, $u_{rel,\,max}/h_s$ and $u_{rel,\,perm}/h_s$, respectively, and the maximum bending moment at the base of the pier, $M_{s,\,max}$, were also plotted against $a_{max,\,inp}$. Figure 7a shows that the FE peak drift plotted close to the linear trend detected in [3] for the centrifuge results. As for the permanent drift, the agreement is even better (Fig. 7b). Lastly, higher bending moments were obtained for the numerical model than all the centrifuge experiments (Fig. 7c), which directly stems from the higher deck acceleration shown in Fig. 6c.

The differences between the FE model and the experimental layout may be mainly attributed to the difference in the initial effective stress profile (Fig. 4a), other than a stiffer sand in the numerical model due to a lack of experimental information. Nonetheless, permanent displacements, which are crucial for designing purposes, were reasonably reproduced in the FE analysis.

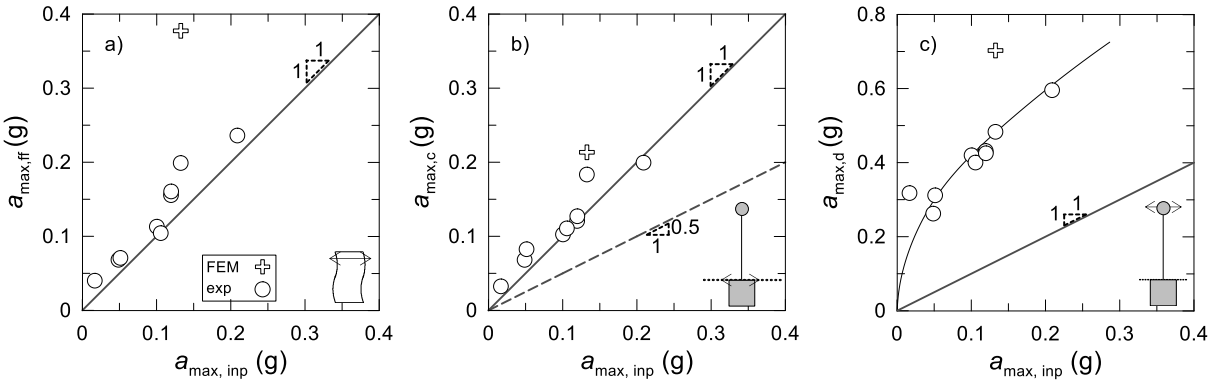

Figure 6: Peak horizontal accelerations recorded at the: (a) far-field ground surface; (b) top of the caisson; (c) deck level.

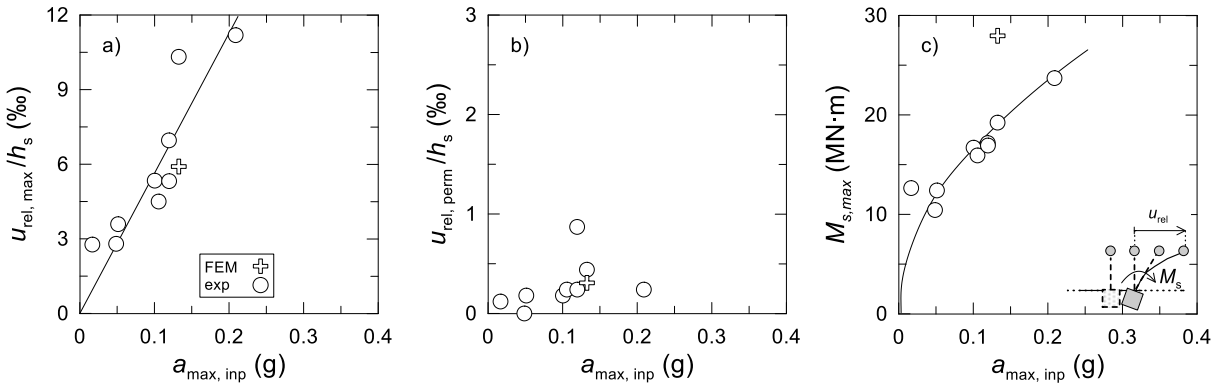

Figure 7: Indices of seismic performance against the peak input acceleration: (a) peak and (b) permanent deck drift; (c) peak bending moment.

5. CONCLUDING REMARKS AND FURTHER DEVELOPMENTS

This paper illustrated the preliminary results of a 3D Finite Element back-analysis reproducing a dynamic centrifuge test where a bridge pier on a caisson foundation, embedded in a soft clay layer, was subjected to a moderate-intensity ground motion. It is shown that it is still possible to fairly capture the seismic performance of the system even when adopting quite a customary constitutive model to describe the mechanical soil behaviour, provided that calibration of soil parameters is carried out in detail. A fair agreement between the numerical and experimental performance indices was obtained indeed, although some differences were actually observed, which may be deemed acceptable at an engineering level though. This result may enhance the reliability of advanced numerical analysis to be performed in the practice when critical infrastructures, such as long-span bridges, are to be designed.

Analyses with different intensity levels have been currently carried out to simulate the series of input motion which were applied in the centrifuge. Softer soil conditions will also be discussed in the next future to assess the predictability of the FE model when soil plasticity is triggered, and bearing capacity of the soil-caisson system is temporarily attained, which were not involved in the case discussed in this paper.

ACKNOWLEDGEMENTS

The numerical analyses were performed thanks to the support by Bentley and Dr. Sandro Brasile. The authors also extend their appreciation to Prof. Gabriele Della Vecchia for his valuable supervision.

REFERENCES

[1] N. Gerolymos, A. Zafeirakos, K. Karapiperis, Generalized failure envelope for caisson foundations in cohesive soil: static and dynamic loading. *Soil Dynamics and Earthquake Engineering*, **78**, 154-174, 2015.

[2] A. Rosati, D. Gaudio, C. di Prisco, S. Rampello, Use of interaction domains for a displacement based design of caisson foundations. *Acta Geotechnica*, **18** (1), 445-468, ISSN: 1861-1125, 2023, DOI: 10.1007/s11440-022-01547-z

[3] D. Gaudio, S.P.G. Madabhushi, S. Rampello, G.M.B. Viggiani, Experimental investigation of the seismic performance of caisson foundations supporting bridge piers. *Géotechnique*, Thomas Telford Ltd, 1-16, 2022, ISSN: 0016-8505, DOI: 10.1680/jgeot.22.00076

[4] I. Anastasopoulos, G. Gazetas, M. Loli, M. Apostolou, N. Gerolymos, Soil failure can be used for seismic protection of structures. *Bulletin of Earthquake Engineering*, **8** (2), 309-326, 2010, DOI: 10.1007/s10518-009-9145-2

[5] D. Gaudio, S. Rampello, The influence of soil plasticity on the seismic performance of bridge piers on caisson foundations. *Soil Dynamics and Earthquake Engineering*, **118**, 120-133, 2019, DOI: 10.1016/j.soildyn.2018.12.007

[6] A. Pecker, Development of the second generation of eurocode 8 – part 5: A move towards performance-based design. F. Silvestri & N. Moraci eds. *7th International Conference on Geotechnical Earthquake Engineering,* Rome, Italy, June 17-20, 273–281, 2019.

[7] Bentley, Plaxis 3D Connect Edition v22 – Reference Manual. Delft University of Technology. Delft, The Netherlands, 2022.

[8] D. Gaudio, S. Rampello, G.S.P. Madabhushi, G.M.B. Viggiani, The role of seismic intensity on the performance of caisson foundations supporting bridge piers: preliminary results from dynamic centrifuge testing. In *Proc. of the 3rd International Conference on Natural Hazard & Infrastructure (ICONHIC 2022)*, Athens, Greece, July 5-7, 2022.

[9] A.N. Schofield, Cambridge Geotechnical Centrifuge Operations. *Geotechnique*, **30** (3), 227-268, 1980, DOI: 10.1680/geot.1980.30.3.227

[10] A.J. Brennan, S.P.G. Madabhushi, Design and performance of a new deep model container for dynamic centrifuge testing. R. Philips, P. Guo, and R. Popescu eds. *International Conference on Physical Modelling in Geotechnics (ICPMG 2002)*, Rotterdam: Balkema, 183-188, 2002.

[11] D. Gaudio, J. Seong, S. Haigh, G.M.B. Viggiani, S.P.G. Madabhushi, R. Shrivatsava, R. Veluvolu, P. Padhy, Boundary effects on dynamic centrifuge modelling of onshore wind turbines on liquefiable soils. *International Journal of Physical Modelling in Geotechnics*, ICE Publishing, **23** (1), 16-34, 2023, ISSN: 1346-213X, DOI: 10.1680/jphmg.21.00085

[12] R.L. Kuhlemeyer, J. Lysmer, Finite Element Method Accuracy for Wave Propagation Problems. *Journal of the Soil Mechanics and Foundations Division*, ASCE, **99** (5), 421-427, 1973, DOI: 10.1061/jsfeaq.0001885

[13] T. Benz, P.A. Vermeer, R. Schwab, A small-strain overlay model. *International Journal for Numerical and Analytical Methods in Geomechanics*, **33** (1), 25-44, 2009.

[14] D.P. Stewart, M.F. Randolph, A new site investigation tool for the centrifuge. H.-Y. Ko and F. G. McLean eds. *Centrifuge '91: Proceedings of International Conference on Centrifuge Modelling*, Rotterdam, the Netherlands, Balkema, 531–538, 1991.

[15] H.B. Seed, I.M. Idriss, *Soil moduli and damping factors for dynamic response analyses,* Report No. EERC 70-10. Earthquake Engineering Research Centre, University of California, Berkeley, California, 1970.

[16] M. Vucetic, R. Dobry, Effect of soil plasticity on cyclic response. *Journal of Geotechnical Engineering*, **117** (1), 89-107, 1991.

[17] D. Gaudio, S. Rampello, The role of soil constitutive modelling on the assessment of seismic performance of caisson foundations. F. Silvestri & N. Moraci eds. *7th International Conference on Geotechnical Earthquake Engineering,* Rome, Italy, June 17-20, 2574-2582, 2019.